

A New Framework for Microrobotic Control of Motile Cells based on High-Speed Tracking and Focusing

Takeshi Hasegawa, Naoko Ogawa, Hiromasa Oku, and Masatoshi Ishikawa

Abstract—We propose a new framework and novel visual control system for motile cells in three-dimensional (3-D) space. Our goal is to utilize microorganisms as micro-robots in various applications by exploiting galvanotaxis (locomotor response to electrical stimulus) to actuate them. This requires automated motion control of swimming cells in 3-D space; in contrast, our previous work has been limited to 1-D or 2-D motion control on the focal plane. The system is capable of 3-D tracking and control of swimming cells by utilizing a high-speed vision system. A combination of “lock-on” tracking within the focal plane and automated focusing using a Depth-From-Diffraction method executed at 1-kHz frame rate ensures both detailed measurement and a large working space. Experimental results for closed-loop 3-D motion control of *Paramecium* cells trapped within a small 3-D region demonstrate the possibility of using microorganisms as micromachines.

I. INTRODUCTION

In recent years, there has been an increasing demand for measurement and control on the micrometer scale along with the progress made in biotechnology and the emerging interest in engineering on the single-cell level. However, such micro-scale operations require high dexterity under a microscope and are quite difficult even for well-trained operators. Thus, autonomous, multifunctional microrobots have been proposed to assist human operators. However, there are many obstacles in realizing such autonomous microrobots.

Our approach is to utilize naturally occurring micromachines, or microorganisms. These small creatures have acquired sophisticated, high-performance internal sensors and actuators through the course of evolution. If we can develop techniques to control them freely, we can realize multi-purpose, programmable microrobotic systems that are superior to existing micromachine systems. Our goal is to eventually integrate controlled microorganisms and information processing systems, as illustrated conceptually in Fig. 1.

To use microorganisms as microrobots, cell actuation is a key technology. In particular, noncontact and non-invasive methods are desirable. We focus on galvanotaxis of microorganisms, an intrinsic locomotor response toward or away from an external electric stimulus. This suggests the possibility of controlling their motion by adjusting an electric field. In addition, it is convenient to utilize galvanotaxis because the input stimulus can be easily controlled by a

T. Hasegawa is with the Department of Creative Informatics, Graduate School of Information Science and Technology, University of Tokyo, Hongo 7-3-1, Bunkyo-ku, Tokyo, Japan.

N. Ogawa, H. Oku and M. Ishikawa are with the Department of Information Science and Computing, Graduate School of Information Science and Technology, University of Tokyo, Hongo 7-3-1, Bunkyo-ku, Tokyo, Japan.

Corresponding author: T. Hasegawa (Takeshi.Hasegawa@ipc.i.u-tokyo.ac.jp)

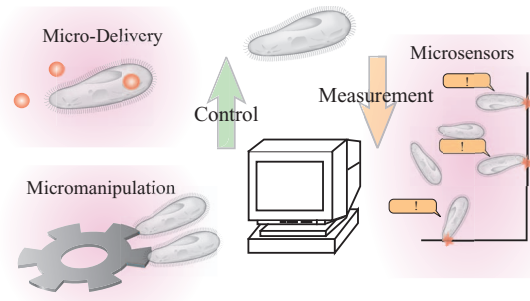


Fig. 1. The concept of our vision: to utilize microorganisms as smart micromachines.

computer system. Fearing and Itoh independently established a firm basis of using microorganisms as machines by galvanotaxis control [1], [2]. Some of the present authors showed improved capabilities by using a high-speed tracking system [3] and demonstrated various applications [4]–[6].

However, all of these previous experiments were performed within a two-dimensional (2-D) horizontal plane. Future advances in motion control of living cells will be indispensable for control of cells in three-dimensional (3-D) space, because it is expected that motion control of cells in 3-D space will greatly enhance the performance of microrobotic applications of motile cells. Though 3-D measurement of cells is necessary for precise visual feedback control in 3-D space, continuous observation of motile cells is difficult because of the particular characteristics of microscope imaging: the shallow depth of field in microscope images restricts clear cell images to within the focal plane only, and motile cells going out of the focal plane will soon disappear from view. At the same time, the working area of cells is restricted to the small field of view of the microscope.

Therefore, we have developed a novel real-time visual-feedback control system for motile cells in 3-D space as a new cell-control framework which can satisfy the requirements of both detailed observation and large 3-D working area. The system executes high-speed 3-D measurement of swimming cells with a tracking microscope and controls their motion by utilizing galvanotaxis. The 3-D tracking consists of two elements, 2-D “lock-on” tracking in the focal plane and focusing along the optical axis using a so-called Depth-From-Diffraction (DFDi) method, as shown in Fig. 2. This paper will describe the system and give experimental results of a 3-D trapping task demonstrating the feasibility of our basic concept, as a first step toward realization of a large-scale microsystem composed of controlled microorganisms.

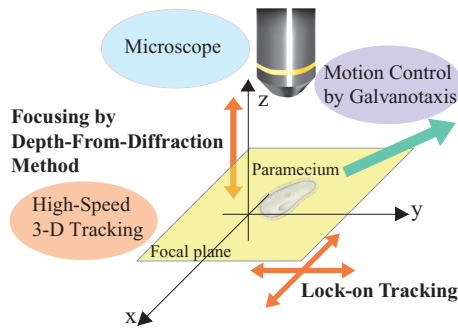


Fig. 2. A new framework for motion control of motile cells in 3-D space. In 2-D lock-on tracking, the camera pursues a target so as to keep it always in the center of the visual field. In DFDi focusing, the focal plane is always set at the target depth.

II. PARAMECIUM AND ITS GALVANOTAXIS

Paramecium caudatum, a kind of protozoa, was used in our cell control experiments. It has an ellipsoidal body from 200 to 250 micrometers in length, and 50 micrometers in width. Its body is covered with cilia, which it beats to swim in water. Paramecium exhibits very strong galvanotaxis [7]; under an external applied electric field, it tends to swim toward the cathode in a spiral manner, as shown in Fig. 3. By using this behavior as a means of actuation, we can control the motion of Paramecium cells.

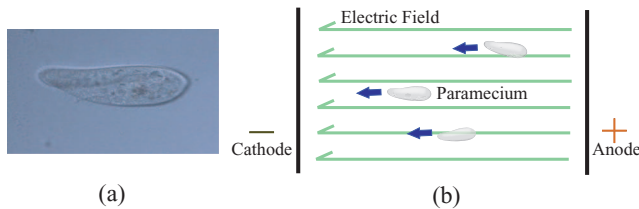


Fig. 3. (a) A Paramecium cell. (b) Galvanotaxis of *Paramecium caudatum*. They tend to swim toward the cathode.

III. TRACKING AND FOCUSING OF SWIMMING CELLS

A. Why High-Speed Tracking and Focusing?

The difficulty in continuous observation of swimming cells using a microscope originates from its small and shallow visual field. For example, a microscope with 10x magnification and 0.25 numerical aperture provides a field of view only 500 μm wide and a depth of field of 7 μm . In comparison, the mean velocity of Paramecium cells is around 1 mm/s. Because of such a shallow depth of field and narrow field of view, cells swimming freely in a large 3-D space can rapidly disappear from the sight within a few milliseconds, thus preventing continuous observation. To overcome this problem, we adopted a kilohertz-order high-speed tracking and focusing system that allows us to continuously observe Paramecium cells in detail in a large working area.

This section describes how the high-speed tracking and focusing of Paramecium cells is performed. We adopted a 2-D lock-on tracking method [8] in the focal plane, and a Depth-From-Diffraction (DFDi) focusing method [9] along

the optical axis. These two technologies allow us to observe swimming cells which are always in focus and in the center of the field of view, and to obtain cell data in real-time. Most previous 3-D tracking systems [10], [11] provided cell data off-line and were not suitable for real-time cell control applications. Moreover, most of them were specially designed for specific targets, thus lacking versatility. Our system has the advantage of being versatile and able to extract various features in real-time.

B. 2-D Lock-On Tracking in the Focal Plane

Lock-on tracking is used to pursue a target so as to keep it always in the center of the visual field [3], [8]. As already shown in Fig. 2, a lock-on mechanism can be realized by moving the position of the specimen on a stage so that the camera always keeps the target at the center.

To track a moving object within the focal plane, we need to know the position of the image centroid of the object. In addition, considering that there may be multiple cells in the field of view, we need to separate each cell and identify the tracking target.

We use a well-known border following algorithm [12] to recognize objects and to obtain their centroids.

1) *How to Obtain Centroids*: The border following algorithm detects objects by tracing their contours using chain codes [12]. A chain code is a way of representing the connection between one pixel and its neighbors on the contour of an object in the image, as shown in Fig. 4. Each pixel on the continuous contour of a given object is in contact with its neighbors. Therefore, any contour can be represented by a connection list of each pixel composing the contour. The connection list is generated by scanning the image and tracing the pixel connections. The centroid of the target cell is calculated from 0-th and 1-st moments of the contour, which are easily obtained through tracing of the contour. This process is executed for each cell in the frame.

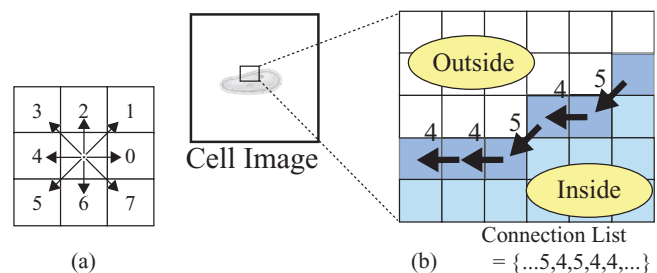


Fig. 4. (a) Chain codes. Connection between a pixel and its 8-neighborhood pixels are represented by a digit from zero to seven. (b) Tracing of the contour using chain codes. The contour can be represented by a connection list.

2) *Identification of the Target Cell*: Identification of the target cell among several cells is realized by choosing the cell closest to the target centroid in the previous frame. This strategy is useful when the frame rate is sufficiently high. Of course, although this method cannot be applied when two objects are overlapped, information about their orientation or velocity would be useful for distinguishing them.

Finally, lock-on tracking is executed by feeding back the obtained information to move the chamber so as to keep the obtained target centroid always at the center of the field.

C. Focusing along the Optical Axis

In the field of microscopy, various methods for autofocusing or 3-D imaging have been proposed. Autofocusing using the spatial frequency of images is one of the principal methods [13]. It is not applicable for real-time control of cells, however, because scanning around the focal plane takes a considerable amount of time.

Thus, we realize focusing by detecting a certain diffraction pattern around the cell in an image to estimate the depth of the cell; this approach is called the Depth-From-Diffraction (DFDi) method [9]. This method allows us to estimate the depth only by a single image and we need not to scan around the focal plane and calculate the spatial frequency.

1) *Depth-From-Diffraction (DFDi) Method:* Consider a cell observed with a microscope under Köhler illumination. When the target cell is in focus, a clear image of the cell is observed. If we adjust the focus slightly to defocus the image, bright and dark diffraction fringes can be observed near the periphery of the cell. For example, Fig. 5 shows these fringes in images of a paramecium cell.

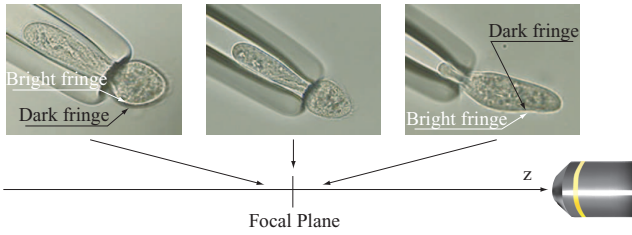


Fig. 5. Diffraction patterns of a Paramecium cell.

We concentrate on two useful characteristics of these fringes: first, the interval of the fringes depends on the distance between the focal plane and the target cell; and second, the sequence of bright and dark fringes depends on the positional relationship between the focal plane and the cell. These characteristics suggest that the depth of the target cell could be estimated from measurement of the fringes.

Since this method can estimate the depth from only a single defocused image, the depth estimation can be performed extremely rapidly. Once the depth is estimated, focusing can be easily realized by moving the specimen into the focal plane.

2) *Depth Displacement Estimation using Image Features:* It is necessary to acquire the precise shape of a target contour because the dark and light fringes located along it must be detected in DFDi. The border-following method described above gives contours of all cells in the image. Then, using intensity patterns along the contour of the target cell, we can estimate the displacement from the focal plane.

Here, we explain how to detect the intensity pattern along the contour. We focus on the fact that the changes of chain codes along the contour indicate the local gradient of the

contour. By detecting an increase or decrease in the chain codes, we can obtain a normal to the contour at a given pixel.

Next, we examine the transition of the pixel intensity through fringe layers that are several pixels thick, along the normal, as shown in Fig. 6. Let us define the average intensity of pixels along the contour as b_0 . The average intensity of pixels along a layer at the Euclidean distance of n pixels from the contour is defined as b_n , as illustrated in Fig.6, where positive n means the outward direction. Various information can be extracted by comparing b_n values for several layers along the contour.

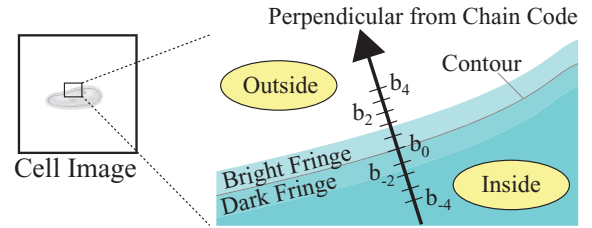


Fig. 6. Definition of image features. The feature b_n indicates the average intensity along the n -th fringe layer from the contour.

From measurement of b_n for a stationary cell at various focus positions, we found that the characteristic index value $i_{abs} = b_2 - b_{-1}$ includes information about the absolute value of displacement, and the values $i_{sgn1} = b_{-4}$ and $i_{sgn2} = b_{-3}$ include information about the sign of the displacement. Fig. 7 shows the distribution of these feature values averaged over four specimens, with respect to the Z position (along with the optical axis) of the focal plane. Because the value i_{abs} is minimized when the displacement Z is around $-20\mu\text{m}$ from the focal plane, a $20\mu\text{m}$ offset was added to the control instruction to the motion stage. In the implementation phase, we estimated the absolute value of displacement sequentially by referring to a quadratic curve fitted to the plot of i_{abs} in Fig. 7.

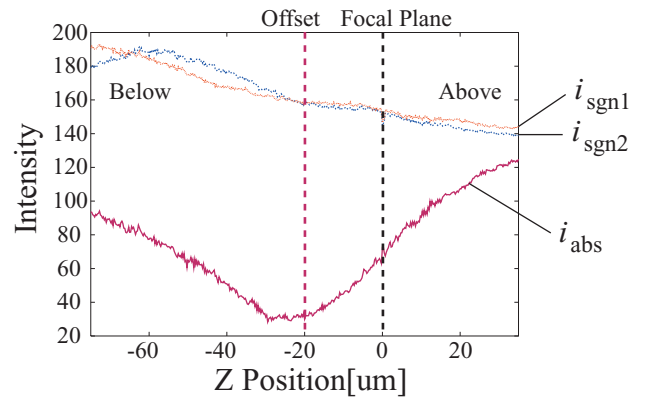


Fig. 7. Image features for estimation of the Z -direction displacement. i_{abs} provides the absolute displacement of the target from the focal plane. i_{sgn1} and i_{sgn2} represent the sign of the displacement.

Because the value i_{abs} provides only the absolute displace-

ment, the system determines if the target is above or below the focal plane by using the values i_{sgn1} and i_{sgn2} . The sign of the displacement is determined to be plus when both i_{sgn1} and i_{sgn2} are less than a certain constant. Thus, we obtain the signed displacement of the target from the focal plane, and the XYZ stage is moved to that focal plane. In our system, the region of $Z = -70\mu\text{m}$ to $+30\mu\text{m}$ was used for focusing.

Thus auto-focusing can be achieved by feeding back image features to move the chamber along the optical axis so that the image is always in focus.

IV. 3-D GALVANOTAXIS CONTROL SYSTEM

A. Overall System Configuration

To realize motion control of Paramecium cells in 3-D space, we developed the novel cell control system shown in Fig. 8. The system consists of an optical microscope, a high-speed vision system, an XYZ automated stage, and two PCs for processing images and controlling the stage.

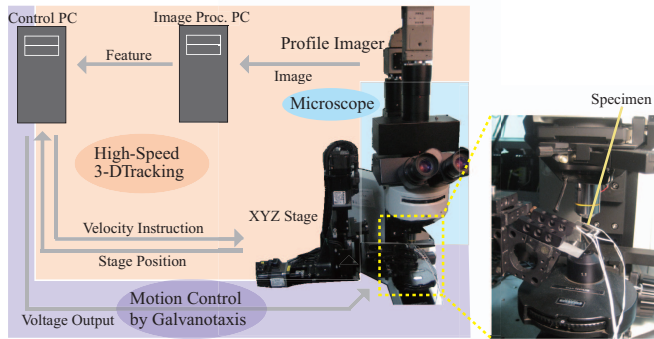


Fig. 8. Configuration and photograph of the system.

The Paramecium cells were kept in a chamber between two pairs of electrodes. The voltage applied to these electrodes is controlled by the PC, yielding galvanotactic motion of Paramecium cells. The high-speed vision system, described below, takes images of the target cell with 1-kHz frame rate and transfers them to the image-processing PC to estimate the 3-D position of the cell in real-time. The XYZ stage is controlled to keep the target cell at the center of the field and in focus. These processes are executed within 1 ms.

B. High-Speed Vision System

As mentioned above, a kilohertz-order frame rate is essential for the vision system, so as not to lose the fast-swimming target. We adopted a high-speed CMOS imager called Profile Imager (Hamamatsu Photonics K. K.) [14]. The frame rate is up to 2,421 frames/s and the resolution is up to 512×512 pixels. In our tracking system, the frame rate was set to about 1 kHz, and the resolution was set to 232×232 pixels. Gray-scale images were converted by a 12-bit A-D converter and transferred to a PC as 8-bit data. In our system, the Profile Imager was mounted on an upright optical microscope (BX50WI, OLYMPUS) and captured bright-field images at 10x magnification.

Images captured by the Profile Imager were transferred to the image-processing PC (Windows XP, Xeon dual 3.0 GHz), where they were processed within 1 ms. A thread for image-processing was executed at 1 kHz using Windows Multimedia Timer API. The thread removed the fixed pattern noise, binarized the image, extracted contours of the cell, and calculated 0-th and 1st moments of all cells in the image using the border-following method. The obtained data was stored in a shared memory (Interface, LPC-4931) to allow it to be shared between the image-processing PC and the stage-control PC. The XYZ stage was controlled to keep the target cell at the center of the field and in focus. These processes were executed within 1 ms.

C. Chamber and 3-D Electrical Field

1) Formation of Electrical Field Distributed in 3-D Space:

One milestone toward our final goal of controlling cells freely in 3-D space is to generate an arbitrary 3-D electric field, formed by 3-D electrodes. Simply stated, three pairs of electrodes are required to form an arbitrary 3-D electrical field. The electrodes along the optical axis are very difficult to realize, however, because they might cause occlusion and hide cells.

In this paper, we focus on motion control of cells in 3-D space using a two-degree-of-freedom electrical stimulus which is assumed to be linear; generation of an arbitrary 3-D electrical field is left as the next step and is not discussed here. Alternatively, it was possible to tilt the chamber with respect to the focal plane of the microscope, as shown in Fig. 9, so as to realize a 3-D field configuration virtually.

Note that degree-of-freedom (DOF) in this paper means how many independent control inputs are used. Although our experiments described in this paper used only 2-DOF inputs, it is essential that the motion of the cells include a vertical component along the optical axis, which has not been successfully controlled before.

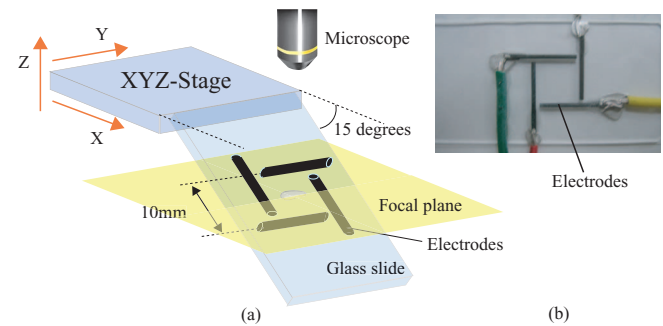


Fig. 9. (a) The chamber with two pairs of electrodes, mounted on an XYZ stage tilted at 15 degrees. Cells swim within the space surrounded by the four electrodes. (b) Photograph of the chamber.

2) Chamber and Electrodes: Fig. 9 shows the electrical stimulus input device. Two pairs of carbon electrodes of 0.9 mm diameter were placed in parallel on a glass slide, so that we could control the electrical stimulus in two directions perpendicular to the electrodes. The distance between them

was 10 mm. Between the electrodes, there was a chamber with a depth of 0.9 mm to contain the specimen. The chamber constrained the motion of the cells within a 3-D space. In order to suppress evaporation of the medium to maintain its depth in the chamber, a cover glass was placed on the chamber.

The voltage applied to these electrodes was controlled by the PC, yielding galvanotactic motion of the Paramecium cells. The PC, running a real-time OS (Pentium 4/3.2GHz, ART-Linux), provided voltage instructions in the range of ± 5 V independently to the electrodes every 1 ms via a D/A converter board (Interface, PCI-3338). By feedback of the image feature values acquired by the Profile Imager, it was possible to control the voltages in real-time according to the target status.

D. XYZ Stage

The chamber was fixed on the XYZ stage (Hephaist, CSZ-080-01) to control its 3-D position with the stage-control PC running a real-time OS (Pentium 4/3.2GHz, ART-Linux). It had three orthogonal axes with 25-mm stroke, as well as X, Y and Z and encoders with 0.25- μ m precision on each axis. All axes were actuated by AC servo motors.

The control program on the PC ran two threads, one for obtaining image moments from the shared memory and the other for controlling the stage, both executed in a 1-kHz process in real-time.

The PC obtained the 3-D error values in the displacement of the target and determined the desired position of the stage in the next step. Using a PID control method, the PC calculated the required velocity instructions and sent them to the servo amplifiers (Mitsubishi Electric, MR-J3). Thus, the stage moved to the desired position, and the target was always located in the center of the visual field and in focus.

V. EXPERIMENTS

In this section, we will describe the experimental results to demonstrate the 3-D control capability of the proposed system using motile cells.

A. Materials

Paramecium caudatum stock 27aG3 cells were adopted as specimens. Cells were cultured at 20-25°C in a solution made with a supplement drink (CalorieMate Can, café au lait flavor, Otsuka Pharmaceutical Co., Ltd.) diluted 400-fold with distilled water, and were grown to the logarithmic or stationary phase (4-10 days after incubation). They were then collected together with the solution, centrifuged to remove debris, and infused into the chamber.

B. 2-DOF Cell Trapping by Depth and Position Control

We performed 2-DOF closed-loop trapping of cells in the 3-D space (Our previous work [15] performed only 1-DOF trapping). In this experiment, simultaneous control of

both the position and depth was attempted. We defined the trapping zone by the following two inequality constraints:

$$\begin{aligned} -250\mu\text{m} < X + Z < 250\mu\text{m}, \\ -250\mu\text{m} < Y < 250\mu\text{m}, \end{aligned}$$

to keep the target cell within this zone. The origin was set to the initial position of the target cell, and the Z direction was along the optical axis. These two constraints were evaluated and adhered to independently to realize 2-DOF control.

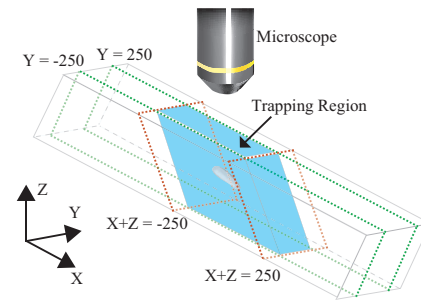


Fig. 10. The coordinate system and the trapping region.

Fig. 11 shows some sequential photographs of a cell as captured by the CCD monitoring camera. The time interval between each image was 0.1 s. The cell was always kept in the center of the image field and in focus, compared to debris in the background.

Fig. 12-15 show results of the control experiment. Fig. 12 shows the time sequence of both the instructed swimming direction by galvanotaxis (green and red arrows) and the sum of the X position and Z position (blue line). The shaded region indicates the trap region. Fig. 13 also shows the time sequence of both the instructed swimming direction by galvanotaxis (green and red arrows) and the Y position (orange line). One can see that the instructed direction was reversed when the cell went out of the region in both plots. Consequently, the cell swam back and forth in the region. Fig. 14 shows the cross-sectional trajectory of the cell within the X-Z plane. The shaded region indicates the trap region as well. The 3-D trajectory of the cell is also shown in Fig. 15.

These results indicate that we achieved continuous closed-loop control of galvanotaxis of motile cells in the 3-D space by tracking. This is an important first step for realizing

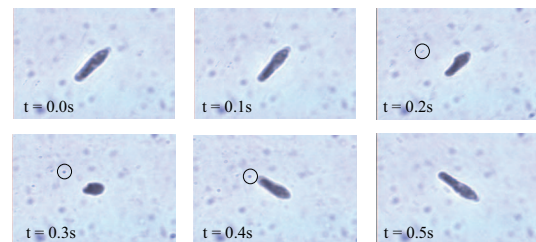


Fig. 11. Sequential photographs of a cell (0.1-s intervals). Debris is indicated by circles.

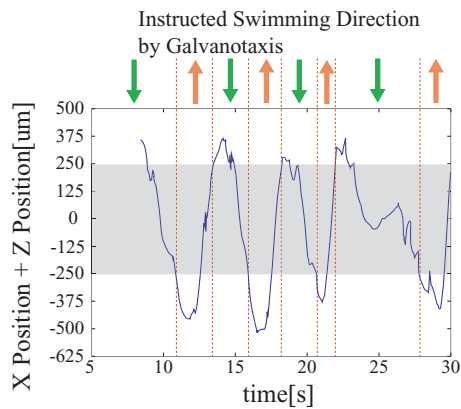


Fig. 12. Instructed swimming direction by galvanotaxis (green and red arrows) and sum of Z position and X position (parallel to the electric field) of a cell (blue line) in 2-DOF trapping experiment. The shaded region is the bounded region for trapping.

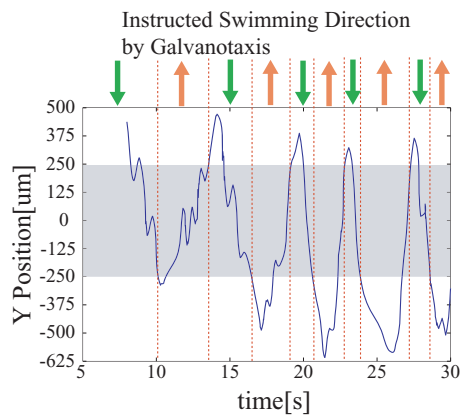


Fig. 13. Instructed swimming direction by galvanotaxis (green and red arrows) and Y position (parallel to the electric field) of a cell (blue line) in 2-DOF trapping experiment. The shaded region is the bounded region for trapping.

a microrobotic system for controlling microorganisms in a wide space.

VI. CONCLUSION

In this paper, we proposed a novel system to control the motion of microorganisms in 3-D space. The system performed high-speed 3-D tracking of cells and actuation of cells using galvanotaxis. Continuous 3-D trapping of *Paramecium caudatum* cells was achieved, which is an important milestone toward the realization of arbitrary cell control for microrobotic applications.

ACKNOWLEDGMENTS

The authors are grateful to Prof. Masaki Ishida of Nara University of Education, Nara, Japan, for supplying the stock 27aG3 *Paramecium* cells.

REFERENCES

- [1] R. S. Fearing, "Control of a micro-organism as a prototype micro-robot," in *Proc. 2nd Int. Symp. Micromachines and Human Sciences*, Oct. 1991.

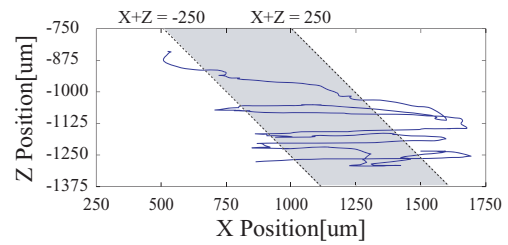


Fig. 14. The cross-sectional trajectory of the cell within the X - Z plane. The shaded region indicates the trap region.

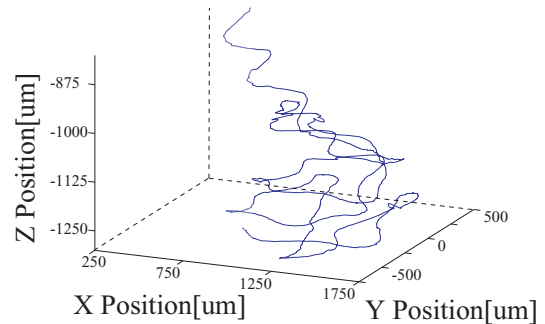


Fig. 15. 3-D trajectory of the controlled cell.

- [2] A. Itoh, "Motion control of protozoa for bio MEMS," *IEEE/ASME Trans. Mechatronics*, vol. 5, no. 2, pp. 181–188, June 2000.
- [3] N. Ogawa, H. Oku, K. Hashimoto, and M. Ishikawa, "Microbotic visual control of motile cells using high-speed tracking system," *IEEE Trans. Robotics*, vol. 21, no. 4, pp. 704–712, Aug. 2005.
- [4] —, "A physical model for galvanotaxis of paramecium cell," *J. Theor. Biol.*, vol. 242, no. 2, pp. 314–328, Sept. 2006.
- [5] N. Ogawa, H. Oku, K. Hashimoto, and M. Ishikawa, "Trajectory planning of motile cell for microrobotic applications," *J. Robotics and Mechatronics*, vol. 19, no. 2, pp. 190–197, Apr. 2007.
- [6] A. Davies, N. Ogawa, H. Oku, K. Hashimoto, and M. Ishikawa, "Visualization and estimation of contact stimuli using living microorganisms," in *Proc. 2006 IEEE Int. Conf. Robotics & Biomimetics (ROBIO 2006)*, Dec. 2006, pp. 445–450.
- [7] H.-D. Görtz, Ed., *Paramecium*. Springer-Verlag, 1988.
- [8] H. Oku, N. Ogawa, K. Hashimoto, and M. Ishikawa, "Two-dimensional tracking of a motile microorganism allowing high-resolution observation with various imaging techniques," *Rev. Sci. Instr.*, vol. 76, no. 3, Mar. 2005.
- [9] H. Oku, Theodoros, M. Ishikawa, and K. Hashimoto, "High-speed autofocusing of a cell using diffraction pattern," *Opt. Expr.*, vol. 14, pp. 3952–3960, May 2006.
- [10] H. C. Berg, "How to track bacteria," *Rev. Sci. Instr.*, vol. 42, no. 6, pp. 868–871, Jun. 1971.
- [11] P. D. Frymier, R. M. Ford, H. C. Berg, and P. T. Cummings, "Three-dimensional tracking of motile bacteria near a solid planar surface," *PNAS*, vol. 92, pp. 6195–6199, Jun. 1995.
- [12] A. Rosenfeld, A. C. Kak, *Digital Picture Processing*. Academic Press, 1976.
- [13] FCA. Groen, IT. Young, G. Lingthart, "A comparison of different focus functions for use in autofocus algorithms," *Cytometry*, vol. 6, pp. 81–91, 1987.
- [14] Y. Sugiyama, M. Takumi, H. Toyoda, N. Mukozaka, A. Ithori, T. Kurashina, Y. Nakamura, T. Tonbe, and S. Mizuno, "A high-speed, profile data acquiring image sensor," in *Dig. Tech. Papers of 2005 IEEE Int. Solid-State Circuits Conf. (ISSCC 2005)*, Feb. 2005, pp. 360–361.
- [15] T. Hasegawa, N. Ogawa, H. Oku, and M. Ishikawa, "Motion Control of Microorganism using High-Speed 3-D Tracking System," in *Proc. 25th Conf. Robotics Society of Japan*, Sept. 2007, 2D12 (in Japanese).